Pergamon

Bioorganic & Medicinal Chemistry 6 (1998) 481–492

BIOORGANIC & MEDICINAL CHEMISTRY

Picrodendrin and Related Terpenoid Antagonists Reveal Structural Differences Between Ionotropic GABA Receptors of Mammals and Insects

Yoshihisa Ozoe,[a,*] Miki Akamatsu,[b] Taizo Higata,[a] Izumi Ikeda,[a] Kazuo Mochida,[a] Kazuo Koike,[c] Taichi Ohmoto[c] and Tamotsu Nikaido[c]

[a]*Department of Life Science and Biotechnology, Shimane University, Matsue, Shimane 690-8504, Japan*
[b]*Division of Environmental Science and Technology, Graduate School of Agriculture, Kyoto University, Kyoto 606-8502, Japan*
[c]*School of Pharmaceutical Sciences, Toho University, Funabashi, Chiba 274-8510, Japan*

Received 25 November 1997; accepted 8 January 1998

Abstract—Twenty-eight picrotoxane terpenoids, including picrodendrins isolated from the Euphorbiaceae plant, *Picrodendron baccatum* (L.) Krug and Urban, have been evaluated for their ability to inhibit the specific binding of [^{3}H]EBOB, the noncompetitive antagonist of ionotropic GABA receptors, to rat-brain and housefly (*Musca domestica* L.)-head membranes. Picrodendrin Q was the most potent competitive inhibitor of [^{3}H]EBOB binding, with IC_{50} values of 16 nM (rat) and 22 nM (*Musca*). We find that the spiro γ-butyrolactone moiety at the 13-position, which contains a carbonyl group conjugated with an unsaturated bond, and the substituents at the 4-position play important roles in the interaction of picrodendrins with their binding site in rat receptors. In contrast, such structural features are not strictly required in the case of the interaction with *Musca* receptors; the spiro saturated γ-butyrolactone moiety at the 13-position, which bears the 16-sp^3 carbon atom, and the hydroxyl groups at various positions are somewhat tolerated. Quantitative structure-activity studies have clearly shown that the electronegativity of the 16-carbon atom and the presence or absence of the 4- and 8-hydroxyl groups are important determinants of the potency of nor-diterpenes in *Musca* receptors, while the negative charge on the 17-carbonyl oxygen atom is likely important in the case of rat receptors. These findings indicate that there are significant differences between the structures of the complementary binding sites in rat GABA receptors and *Musca* GABA receptors. We also infer differences between native *Musca* GABA receptors and the *Drosophila Rdl* subunit-containing homo-oligomeric GABA receptors in the structures of their binding sites.

Introduction

γ-Aminobutyric acid (GABA), an inhibitory neurotransmitter, binds to two major types of receptors, $GABA_A$ (ionotropic) and $GABA_B$ (metabotropic) receptors, to regulate the central nervous system of vertebrates.[1,2] The $GABA_A$ receptor belongs to a family of ligand-gated ion channels composed of hetero-oligomeric subunits,[3] where GABA induces the opening of the channel and Cl^- influx into the nerve cell. More than 100 medicinal and toxic compounds have been reported to act on $GABA_A$ receptors.[4] Insects have similar ionotropic receptors with different pharmacological properties, so that their GABA receptors are promising targets for insecticides.[5]

Picrodendrins are a series of terpenoids recently isolated from the bark and stems of the Euphorbiaceae plant, *Picrodendron baccatum* (L.) Krug and Urban.[6–12] With respect to the economic use of this plant, it has been reported that in the Dominican Republic, leaves of the *Picrodendron*, called 'mata becerro' (calf killer), are reduced to powder and used to kill bedbugs and lice.[13] Meanwhile, some of these terpenoids have been reported

*Corresponding author. Tel: +81-852-32-6573; Fax: +81-852-32-6499; E-mail: ozoe-y@life.shimane-u.ac.jp

0968-0896/98/$19.00
PII: S0968-0896(98)00012-1

to competitively inhibit the specific binding of the noncompetitive GABA antagonist [^{35}S]*t*-butylbicyclophosphorothionate (TBPS) to rat-brain membranes[14] and to depress GABA-induced Cl^- currents in the *Drosophila Rdl* subunit-containing homo-oligomeric GABA receptors.[15] The results of the radioligand-binding and electrophysiological studies indicate that the action of picrodendrins as the noncompetitive antagonist of ionotropic GABA receptors underlies the insecticidal activity of *P. baccatum*.

In the present study, we have assayed picrodendrins and other related terpenoids for their inhibition of the specific binding of the noncompetitive GABA antagonist [^{3}H]4′-ethynyl-4-*n*-propylbicycloorthobenzoate (EBOB) (Figure 1) to rat-brain and housefly (*Musca domestica* L.)-head membranes. Figure 1 illustrates the structures of the 28 terpenoids assayed, comprising nor-diterpenes and sesquiterpenes that are hydroxylated or rearranged at various positions. Picrodendrins share the picrotoxane skeleton with picrotoxinin, a sesquiterpene used as a standard noncompetitive antagonist in basic research on GABA receptors. Furthermore, the nor-diterpenes have a novel, unique skeleton containing a spiro γ-butyrolactone ring, while the sesquiterpenes are considered as analogues of tutin, a known sesquiterpene from Coriariaceae plants. Structure–activity relationship (SAR) studies of these structurally diverse terpenoids might assist in gaining insight into the molecular topography of ionotropic GABA receptors. We report here the results of binding assays, and we infer structural differences in the antagonist binding sites of mammalian and insect GABA receptors.

Results

Effects on [^{3}H]EBOB binding to rat-brain membranes

Twenty-eight terpenoids were evaluated as inhibitors of [^{3}H]EBOB binding to rat-brain membranes. The IC_{50} values are listed in Table 1, and the concentration–inhibition curves are shown in Figure 2. Eight terpenoids inhibited specific [^{3}H]EBOB binding with IC_{50} values of less than 10 μM, and the IC_{50} values of five out of the eight terpenoids were less than 1 μM. Picrodendrin Q, with an IC_{50} value of 16 nM, was the most potent among them, being about 39-fold more potent than the standard terpenoid antagonist picrotoxinin. Scatchard plots indicate that picrodendrin Q binds to a site identical to that of EBOB in rat receptors (Figure 3). Picrodendrin M, which is hydroxylated at the 8-position, was about 9-fold less potent than picrodendrin Q. Hydroxylation at the 4- and 19-positions of picrodendrin Q to give picrodendrin A resulted in an approximately 17-fold loss in potency when compared to picrodendrin Q. Picrodendrin T, the geometrical isomer of picrodendrin A, was about 36-fold and 613-fold less potent than picrodendrin A and Q, respectively. Picrodendrin B, which is unsaturated between the 14- and 16-positions, was among the weak inhibitors, probably because of the presence of a hydroxyl group at the 4-position. Picrodendrin O also exhibited a marked decrease (525-fold) in potency compared to picrodendrin Q, although they differ only in the substitution pattern at the 16-position. Hydroxylation at the 8-position of picrodendrin O to give picrodendrin E resulted in an almost complete loss of activity. Dihydrotutin, a sesquiterpene bearing an isopropyl group at the 4-position, was an approximately 281-fold less potent inhibitor than picrodendrin Q. Replacement of the isopropyl group with an isopropenyl or a hydroxyisopropyl group led to an approximately 5-fold increase or a substantial loss of activity, respectively (tutin and isohyenanchin).

Effects on [^{3}H]EBOB binding to *Musca*-head membranes

Fifteen of the 28 terpenoids exhibited a concentration-dependent inhibition of specific [^{3}H]EBOB binding to *Musca*-head membranes, with IC_{50} values of less than 10 μM (Table 1, Figure 4). Ten out of the 15 terpenoids had IC_{50} values of less than 1 μM. Picrodendrin Q was the most potent inhibitor in the *Musca* receptors as well, with an IC_{50} value (22 nM) similar to that in rat receptors. Picrodendrin Q was more potent than picrotoxinin only by 4-fold, in contrast to a 39-fold difference in rat receptors. Inhibition of [^{3}H]EBOB by this terpene was competitive here too (Figure 3). Picrodendrin B, E, F, G, L, P, and corianin exhibited IC_{50} values in the 0.3–4 μM range in *Musca* receptors, although they were inactive or weakly active in rat receptors (IC_{50} > 10 μM). Differences in potency among the terpenoids tended to be small compared to those in rat receptors. Picrodendrin M, A, T, O, E, and dihydrotutin were approximately 7-, 31-, 118-, 5-, 45-, and 30-fold less potent than picrodendrin Q, respectively. Picrodendrin A was only 4-fold more potent than picrodendrin T in *Musca* receptors, while being 36-fold more potent in rat receptors.

In vivo effects on cockroaches

To explore the correlation of in vitro and in vivo activities, 21 terpenoids were examined for their insecticidal effects. Seven out of the 21 tested terpenoids were insecticidal against German cockroaches (*Blattella germanica* L.), with LD_{50} values of less than about 1 μg/roach, when injected after topical treatment of cockroaches with piperonyl butoxide, a mixed-function oxidase inhibitor (Table 1). Picrodendrin M and Q were highly active, with LD_{50} values of 47 ng (0.11 nmol)/

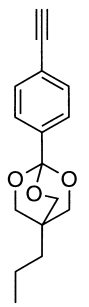

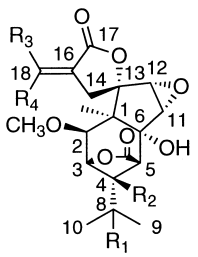

	R_1	R_2	R_3	R_4
PD-A:	H	OH	CH_2OH	OCH_3
PD-M:	OH	H	CH_3	OCH_3
PD-Q:	H	H	CH_3	OCH_3
PD-T:	H	OH	OCH_3	CH_2OH

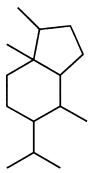

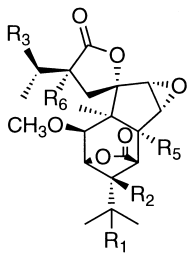

	R_1	R_2	R_3	R_5	R_6
PD-E:	OH	H	OH	OH	H
PD-E-18-Ac:	OH	H	$OCOCH_3$	OH	H
PD-F:	H	OH	OH	OH	OH
PD-L:	H	OH	OH	H	OH
PD-O:	H	H	OH	OH	H

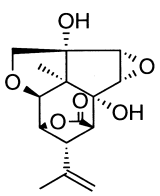

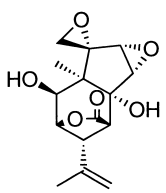

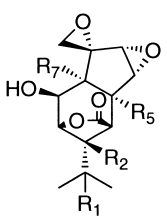

	R_1	R_2	R_5	R_7
PD-C:	H	OH	OH	CH_3
PD-D:	H	OH	H	CH_3
PD-I:	H	OH	H	CH_2OH
PD-J:	OH	OH	OH	CH_3
Dihydrotutin:	H	H	OH	CH_3
Isohyenanchin:	OH	H	OH	CH_3

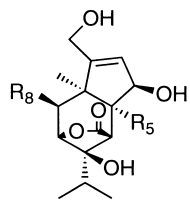

	R_5	R_8
PD-H:	OH	OCH_3
PD-α:	H	OH

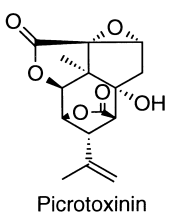

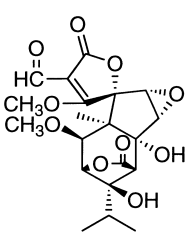

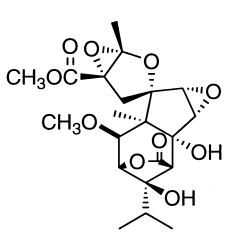

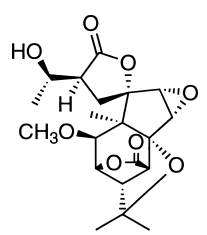

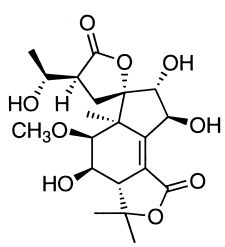

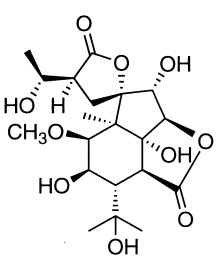

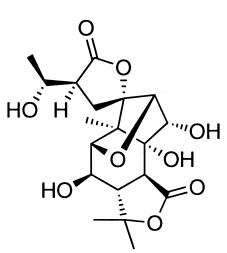

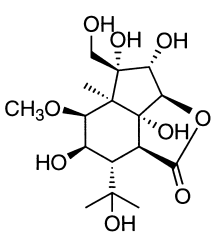

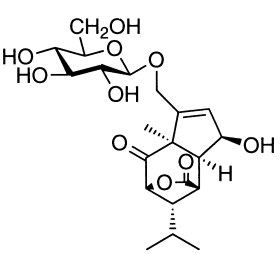

Figure 1. Structures of picrotoxane terpenoids and EBOB. Abbreviations of the terpenoids' names are defined in Table 1. PS refers to the picrotoxane skeleton. The numbering system shown on the structures of picrodendrin A, M, Q, and T is based on ref 6.

roach and 71 ng (0.17 nmol)/roach, respectively, and the other four terpenoids were moderately active.

Quantitative SAR studies

Traditional quantitative SAR analysis was carried out to identify the major determinants of potency of nor-diterpenes containing a spiro γ-butyrolactone at the 13-position. Because the substitution patterns at the 4-, 8- and 16-positions appeared to be quite important, the following parameters were used as independent variables in the present analysis: charges on the 16-, 17-carbon atoms (C16_ch, C17_ch) and the 17-carbonyl oxygen atom (C17O_ch), and an indicator variable for the presence or absence of the hydroxyl group at either the 4- or 8-position (C48_OH). As a result of an analysis of the binding data for the *Musca* receptors, eq (1) was obtained for the 12 picrodendrins listed in Table 2.

$$\log(1/IC_{50}(M)) = -2.870(\pm 2.231)C16\_ch - 1.419(\pm 0.753)C48\_OH + 6.933(\pm 0.744) \quad (1)$$

$$n = 12, s = 0.427, r = 0.877, F_{2,9} = 14.947$$

In this equation, n is the number of data points, s is the standard deviation, r is the correlation coefficient, and F is the value of the F-test. The figures in parentheses are the 95% confidence intervals. Considering that the contributions of other parts of the nor-diterpenes were neglected in the analysis, the correlation coefficient (0.877) is satisfactory. The difference between the measured and calculated potency values for picrodendrin E-18-acetate was largest (Table 2), suggesting a negative

Table 1. Potencies of picrodendrins and related terpenoids in inhibiting [^{3}H]EBOB binding and their insecticidal activities

Terpenoid	[^{3}H]EBOB binding, IC_{50}(μM)		Insecticidal activity, LD_{50}(μg/roach)
	Rat	*Musca*	*Blattella*
PD-A	0.27 ± 0.04[a]	0.69 ± 0.34[a]	1.1 (0.90–1.2[b])
-B	13 ± 1[a]	0.35 ± 0.11[a]	> 1 (20[c])
-C	> 10 (33 ± 2[d])	12 ± 4[a]	> 1 (15[c])
-D	> 10 (12 ± 4[d])	> 10 (40 ± 10[d])	> 1 (5[c])
-E	> 10 (20 ± 9[d])	0.99 ± 0.54[a]	> 1 (10[c])
-E-18-Ac	> 10 (9 ± 1d)	13 ± 1[a]	> 1 (0[c])
-F	> 10 (3 ± 2[d])	3.1 ± 0.8[a]	> 1 (5[c])
-G	> 10 (6 ± 3[d])	3.9 ± 0.4[a]	> 1 (43[c])
-H	> 10 (6 ± 12[d])	> 10 (29 ± 1[d])	—[e]
-I	> 10 (2 ± 2[d])	> 10 (25 ± 11[d])	> 1 (0[c])
-J	> 10 (1 ± 1[d])	> 10 (2 ± 6[d])	> 1 (0[c])
-L	> 10 (4 ± 6[d])	3.5 ± 1.6[a]	> 0.25 (0[c])
-M	0.15 ± 0.02[a]	0.15 ± 0.05[a]	0.047 (0.043–0.052[b])
-O	8.4 ± 3.4[a]	0.11 ± 0.05[a]	0.37 (0.24–0.57[b])
-P	> 10 (6 ± 1[d])	2.8 ± 1.5[a]	> 1 (40[c])
-Q	0.016 ± 0.004[a]	0.022 ± 0.002[a]	0.071 (0.065–0.078[b])
-T	9.8 ± 2.3[a]	2.6 ± 0.7[a]	> 1 (5[c])
-U	> 10 (1 ± 8[d])	> 10 (4 ± 2[d])	—[e]
-X	> 10 (−1 ± 4[d])	> 10 (4 ± 5[d])	—[e]
-Y	> 10 (19 ± 0[d])	> 10 (28 ± 6[d])	—[e]
-Z	> 10 (−1 ± 2[d])	> 10 (14 ± 11[d])	—[e]
-α	> 10 (−6 ± 2[d])	> 10 (8 ± 3[d])	—[e]
PDside A	> 10 (−5 ± 3[d])	> 10 (2 ± 6[d])	—[e]
Tutin	0.95 ± 0.16[a]	0.43 ± 0.12[a]	0.84 (0.75–0.94[b])
DHtut	4.5 ± 1.1[a]	0.65 ± 0.23[a]	> 1 (20[c])
Corianin	> 10 (31 ± 11[d])	0.33 ± 0.02[a]	0.11 (0.09–0.13[b])
Isohyen	> 10 (14 ± 6[d])	> 10 (48 ± 0[d])	> 1 (5[c])
PTX	0.62 ± 0.11[a]	0.091 ± 0.001[a]	0.41 (0.35–0.49[b])

[a] Mean ± SD.
[b] 95% confidence limit.
[c] Mortality (%) at indicated dosages.
[d] Inhibition (%) at 10 μM.
[e] Not determined.
Abbreviations: PD-A to -α, picrodendrin A to α; PD-E-18-Ac, picrodendrin E-18-acetate; PDside A, picrodendriside A; DHtut, dihydrotutin; Isohyen, isohyenanchin; PTX, picrotoxinin.

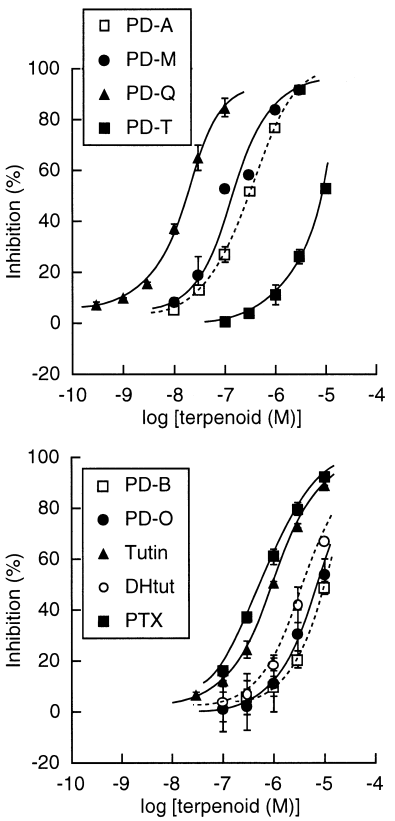

Figure 2. Concentration–inhibition curves of picrotoxane terpenoids for specific [^{3}H]EBOB binding to rat-brain membranes. Abbreviations of the terpenoids' names are defined in Table 1.

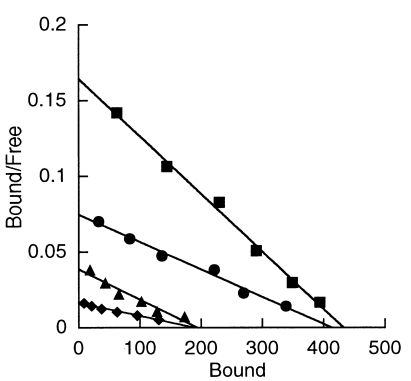

Figure 3. Scatchard plots of [^{3}H]EBOB binding to rat-brain and *Musca*-head membranes in the absence and presence of picrodendrin Q. ■, rat, without PD-Q; ●, rat, with 16 nM PD-Q; ▲, *Musca*, without PD-Q; ◆, *Musca*, with 22 nM PD-Q. Bound, [^{3}H]EBOB bound specifically to membranes (fmol/0.125 mg protein (rat) or fmol/0.25 mg protein (*Musca*)); Free, free [^{3}H]EBOB (fmol). Values are the mean of triplicate determinations, and the graph is typical of two similar experiments.

effect of the acetyl group at the 18-position. In the analysis for the 11 compounds, except for picrodendrin E-18-acetate, the correlation quality was improved ($s = 0.345$, $r = 0.912$, equation not shown). Equation (1) indicates that the potency of nor-diterpenes increases in the presence of a more negative charge on the 16-carbon atom and in the absence of hydroxyl groups at the 4- and 8-positions. In the case of rat receptors, the number of active nor-diterpenes was not enough to perform a detailed analysis. However, it should be noted that potent picrodendrins (A, M, and Q), with an IC_{50} value of less than 1 μM, had highly negative charges (< -3) on the 17-carbonyl oxygen atom (Table 2).

Discussion

SAR in rat $GABA_A$ receptors

Picrodendrins and other related terpenoids have previously been demonstrated to competitively inhibit specific [^{35}S]TBPS binding to rat-brain membranes.[14] In the present study, [^{3}H]EBOB was used to explore the interaction of the terpenoids with insect GABA receptors as well as mammalian GABA receptors, since [^{3}H]EBOB has been shown to be preferred over [^{35}S]TBPS when applied to insect receptors.[16] Both binding assays using different radioligands gave similar results in rat receptors, as can be judged from the good correlation between the log IC_{50} values of seven active terpenoids in inhibiting specific [^{35}S]TBPS and [^{3}H]EBOB binding to rat-brain membranes ($r = 0.991$, plots not shown).

In both cases, picrodendrin Q was found to be more potent than picrotoxinin and the most potent among the terpenoids assayed to date. As exemplified by the activities of isohyenanchin, picrodendrin M, and E, which were lower than those of dihydrotutin, picrodendrin Q, and O, respectively, the hydroxyl group at the 8-position appears to exert a negative effect on receptor binding. The isopropyl or isopropenyl group *trans* to the lactone moiety connecting the 3- and 5-positions of the skeleton exerts positive effects on receptor binding, as has been shown with the *cis* and *trans* isomers of a caged lactone bearing a partial skeleton of picrotoxinin.[17] As for the substituent at the 4-position, an isopropenyl group is preferred over an isopropyl group in rat receptors, as shown by the approximately 5-fold higher potency of tutin than dihydrotutin. This suggests that the electronic nature of the 4-substituent might be favorable for the interaction of sesquiterpenes with rat receptors. Terpenoids containing a lactone ring bridging the 2- and 13-positions (picrotoxinin), a spiro epoxide at the 13-position (dihydrotutin, tutin), and a spiro α-ethyl-γ-butyrolactone at the 13-position (picrodendrin O) were active in rat receptors only when they were not hydroxylated

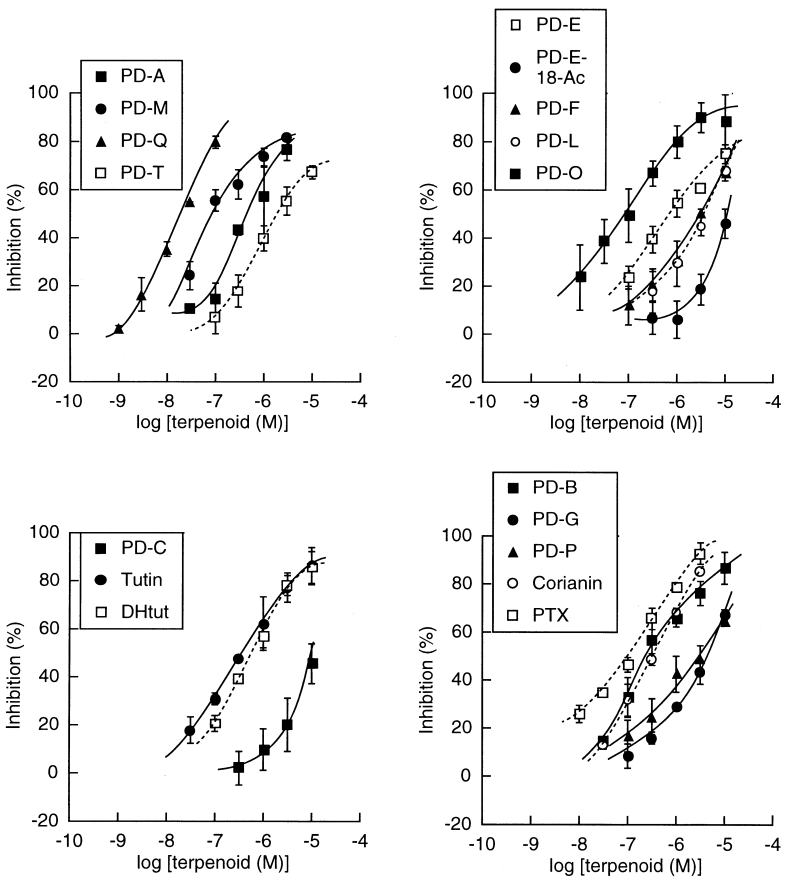

Figure 4. Concentration–inhibition curves of picrotoxane terpenoids for specific [^{3}H]EBOB binding to *Musca*-head membranes. Abbreviations of the terpenoids' names are defined in Table 1.

Table 2. Biological data, physicochemical parameters, and an indicator variable

Terpenoid	log(1/IC_{50}(M))				C16_ch[a]	C17_ch[b]	C17O_ch[c]	C48_OH[d]
	Rat (Obsd)	*Musca*						
		Obsd	Calcd	Dev				
PD-A	6.57	6.16	6.131	0.029	−0.215	0.379	−0.312	1
-B	4.89	6.46	6.441	0.019	−0.323	0.385	−0.265	1
-E	—[e]	6.00	5.626	0.374	−0.039	0.333	−0.298	1
-E-18-Ac	—[e]	4.89	5.672	−0.782	−0.055	0.335	−0.294	1
-F	—[e]	5.51	5.258	0.252	0.089	0.349	−0.273	1
-G	—[e]	5.41	5.588	−0.178	−0.026	0.170	—[f]	1
-L	—[e]	5.46	5.264	0.196	0.087	0.346	−0.273	1
-M	6.82	6.82	6.137	0.683	−0.217	0.381	−0.316	1
-O	5.08	6.96	7.065	−0.105	−0.046	0.339	−0.296	0
-P	—[e]	5.55	5.637	−0.087	−0.043	0.329	−0.293	1
-Q	7.80	7.67	7.565	0.105	−0.220	0.380	−0.316	0
-T	5.01	5.59	6.096	−0.506	−0.203	0.382	−0.279	1

[a–c]Charges on the 16- and 17-carbon atoms, and that on the 17-carbonyl oxygen atom, respectively.
[d]Indicator variable for the presence or absence of the hydroxyl group at the 4- or 8-position.
[e] Not determined ($IC_{50} > 10\,\mu M$).
[f]Not determined because of the absence of the 17-carbonyl oxygen atom.
Abbreviations of the terpenoids' names are defined in Table 1.

at both the 4- and 8-positions. However, picrodendrin A, B, M, and T retained activity, despite carrying such deleterious hydroxyl groups. These terpenoids bear a spiro α-ethylidene-γ-butyrolactone or a spiro α,β-unsaturated γ-butyrolactone at the 13-position. The presence of the 17-carbonyl group conjugated with an unsaturated bond is most likely responsible for their relatively high potency. The calculation of the atomic charges of this moiety led us to speculate that the highly negative charge of the 17-carbonyl oxygen might result in the high potency of picrodendrin A, M, and Q (Table 2). The potency of picrodendrin T, which was lower than that of its geometrical isomer, picrodendrin A, could be explained by the poor negative charge of its 17-carbonyl oxygen atom. Although corianin and picrodendriside A have no hydroxyl groups at the 4- and 8-positions, they were almost inactive, probably because other parts were either detrimental to activity or insufficient.

SAR in *Musca* GABA receptors

With the exception of picrodendrin A, M, and Q, the terpenoids tested were more potent in *Musca* receptors than in rat receptors (Figure 5, Table 1). In particular, picrodendrin B, O, and corianin proved to be about 37-, 76-, and at least 30-fold more selective inhibitors for *Musca* receptors than for rat receptors, respectively. Also, picrodendrin B, E, F, G, L, P, and corianin were moderately active in *Musca* receptors, though inactive or weakly active in rat receptors. The spiro α-ethyl-γ-butyrolactone ring at the 13-position and the hydroxyl groups at various positions were better tolerated in *Musca* receptors than in rat receptors. Quantitative SAR analysis has clearly demonstrated that the electro-

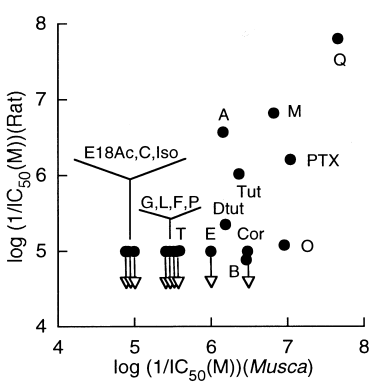

Figure 5. Relationships between the potencies of picrotoxane terpenoids in inhibiting [^{3}H]EBOB binding to rat-brain and *Musca*-head membranes. Arrows indicate that the compounds have IC_{50} values of $>>10\,\mu M$. A–O, E-18Ac, Tut, Dtut, Iso, Cor, and PTX refer to picrodendrin A–O, picrodendrin E-18-acetate, tutin, dihydrotutin, isohyenanchin, corianin, and picrotoxinin, respectively.

negativity of the 16-carbon atom and the presence or absence of the 4- and 8-hydroxyl groups are important determinants of the potency of nor-diterpenes. It is noteworthy that the negative charge on the 16-carbon atom appears to make a great contribution to the high potency in *Musca* receptors, while the negative charge on the 17-carbonyl oxygen atom makes this contribution in the case of rat receptors. This difference might reflect a difference between rat and *Musca* receptors in the structures of their binding sites. Although tutin analogues with hydroxyl group(s) at the 4-, 8-, or both positions (picrodendrin C, D, I, J, and isohyenanchin) were inactive or only weakly active in *Musca* receptors as in rat receptors, those lacking such a hydroxyl group (tutin, dihydrotutin, and corianin) were almost equally potent in *Musca* receptors, in contrast to big differences in their potency in rat receptors. These findings indicate that the hydrophobic properties of the 4- and 8-positions are of critical importance in the interaction between tutin analogues and *Musca* receptors. All active compounds in *Musca* receptors, as well as in rat receptors, had a lactone ring connecting the 3- and 5-positions of the skeleton. More analogues need to be assayed to determine whether this moiety is essential to activity.

Three-dimensional binding-site model

We have previously proposed a model of the binding site of noncompetitive $GABA_A$ receptor antagonists,[18] using CoMFA (comparative molecular field analysis), which is a procedure for three-dimensional quantitative SAR analyses.[19] Picrodendrin Q was aligned according to the binding-site model, and the superposition of EBOB on picrodendrin Q is shown in Figures 6–9. Based on this alignment, the CoMFA was made for the activity in inhibiting [^{35}S]TBPS binding to the rat receptors of 27 compounds (see refs 14 and 18 for data), including picrodendrin A, B, M, O, and Q, together with the series 1 GABA antagonists used in our previous study.[18] The CoMFA method used was similar to that described in a previous paper.[18] Although a significant equation (the crossvalidated correlation coefficient, $q^2 > 0.3$) was not obtained because the number of picrodendrin derivatives used in the analysis was small, the q^2 in the equation obtained was fairly high (0.255). The superposition of picrodendrins and the GABA antagonists as well as the CoMFA for the combined set of these compounds is still under investigation.

We attempted to qualitatively explain the SAR for picrodendrin derivatives using the above most probable alignment and the CoMFA contour maps generated in our previous study.[18] Figures 6 and 7 represent the overlay of the structures of picrodendrin Q and EBOB with the major steric and electrostatic-potential contour maps, respectively, drawn according to the CoMFA

equation for *Musca* GABA receptors. Figures 8 and 9 show the compounds with the steric and electrostatic contour maps, respectively, according to the equation for rat receptors. The green areas in Figures 6 and 8 indicate regions where the submolecular bulk is well accommodated with an increase in activity, whereas the yellow areas indicate regions where the submolecular bulk is unfavorable to the activity. The red areas in Figures 7 and 9 indicate regions where the more negative electrostatic interaction with the receptor binding site increases the activity, whereas the blue areas show regions where the reverse is the case. As shown in Figures 6–9, the 16-carbon atom of picrodendrin Q is located close to the 1-carbon atom of the benzene ring of EBOB, while the 17-carbonyl oxygen atom is close to the 2- or 6-carbon atom (one of the *ortho*-carbon atoms). In Figures 7 and 9, the negative electrostatic-potential regions of ligands that interact with *Musca* and rat receptors appear below the 1-carbon atom and around an *ortho*-position, respectively, of the benzene ring of EBOB. This finding seems to be in agreement with the results of the quantitative SAR analysis, which indicates the importance of the negative atomic charges on the 16-carbon atom for the activity in *Musca* receptors while that on the 17-carbonyl oxygen atom in rat receptors.

Figure 6 shows the region above the benzene ring of EBOB in which the steric bulk of the ligand substructure is unfavorable in *Musca* receptors, whereas in rat receptors sterically unfavorable regions appear not only above but also below the benzene ring (Figure 8). The 16-hydrogen atom in picrodendrins that bear the sp^3 16-carbon atom (picrodendrin E, F, L, O, and P) invades the unfavorable region above the benzene ring in *Musca* receptors (stereoviews not displayed) and probably therefore lowers their activity compared to picrodendrin Q. In the case of rat receptors, the nonplanar substituents as well as the hydrogen atom at the 16-position protrude into the sterically unfavorable regions, so the compounds except picrodendrin O might show no measurable activity.

In Figure 8, the 8-hydroxyl group of picrodendrin E and M could be located close to the sterically favorable region around the hydrophobic *n*-propyl group of EBOB. Assuming that the hydrophobic interaction of

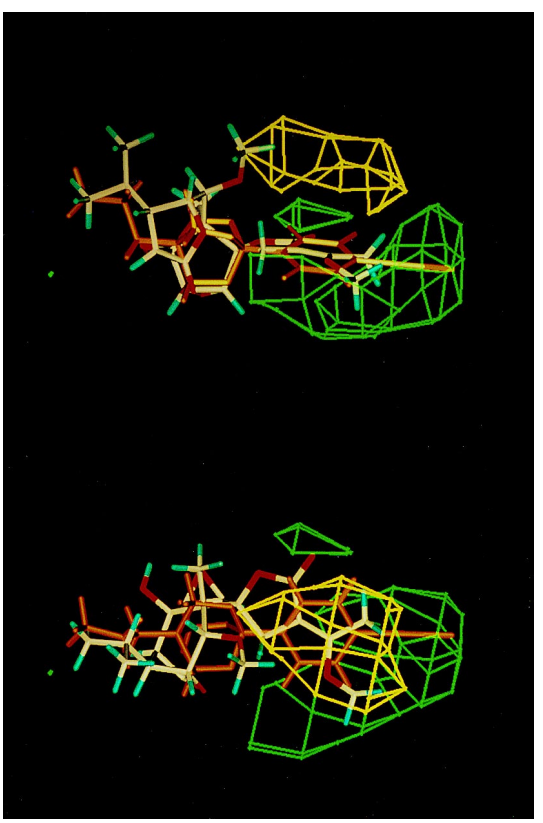

Figure 6. Orthogonal views of contour diagrams of the steric fields according to the CoMFA equation for *Musca* receptors with picrodendrin Q and EBOB (orange). See the text for explanations of the colors of the fields.

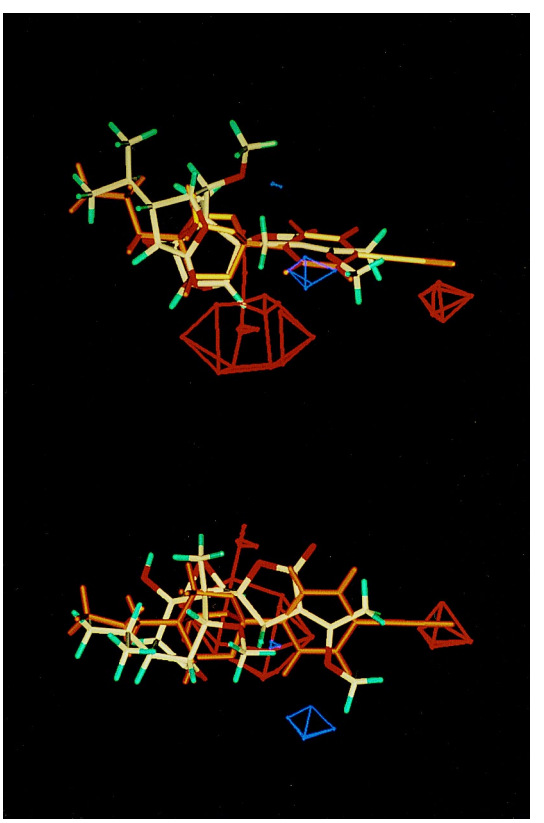

Figure 7. Orthogonal views of contour diagrams of the electrostatic fields according to the CoMFA equation for *Musca* receptors with picrodendrin Q and EBOB (orange).

substituents with receptors is favorable in this region,[20] it is likely that the hydrophilic hydroxyl group decreases the activity of picrodendrin E and M compared to picrodendrin O and Q, respectively. This region does not seem to be of critical importance in *Musca* receptors, as shown in Figure 6. Regarding the 4-position, no suggestion was obtained from this superposition and the CoMFA regions in Figures 6–9.

Probing ionotropic GABA receptors of insects

To date, three genes encoding ionotropic GABA receptor-like subunits have been cloned from grape fruit flies (*Drosophila melanogaster* Meig.).[21–23] One of the gene products (*Rdl*) has been reported to form a functional homo-oligomeric receptor that shares some pharmacological properties with native receptors.[24,25] *Rdl* homologues have been identified in other insect species including *M. domestica*,[26] suggesting that the *Rdl* subunit is a component of many insect GABA receptors. The antagonist actions of picrodendrin and tutin analogues have been electrophysiologically examined on *Drosophila Rdl* homo-oligomers expressed in *Xenopus* oocytes.[15] In comparing the results of the electrophysiological studies with those obtained in the present studies, several differences are evident between the potencies of the terpenoids as inhibitors of [^{3}H]EBOB binding in native *Musca* receptors and as blockers of GABA-induced Cl^- currents in *Drosophila Rdl* homo-oligomeric receptors (Figure 10). Picrodendrins (A, B, F, and G) with a hydroxyl group at the 4-position were approximately 10- to 28-fold more potent in cloned *Rdl* receptors than in native *Musca* receptors, while picrodendrins (O and Q) without such a hydroxyl group were less active in *Rdl* receptors or equipotent between both receptors. Tutin analogues were approximately 2- to 7-fold less potent in *Rdl* receptors than in *Musca* receptors, regardless of the presence of the 4-hydroxyl group. Potencies in the *Rdl* receptors of tutin, dihydrotutin, and isohyenanchin, which differ only in the substituent at the 4-position, were parallel with potencies in rat receptors rather than those in *Musca* receptors.

As shown in Figure 11, the correlation of the insecticidal (in vivo) activity against B. *germanica* with the inhibitory (in vitro) activity of [^{3}H]EBOB binding on

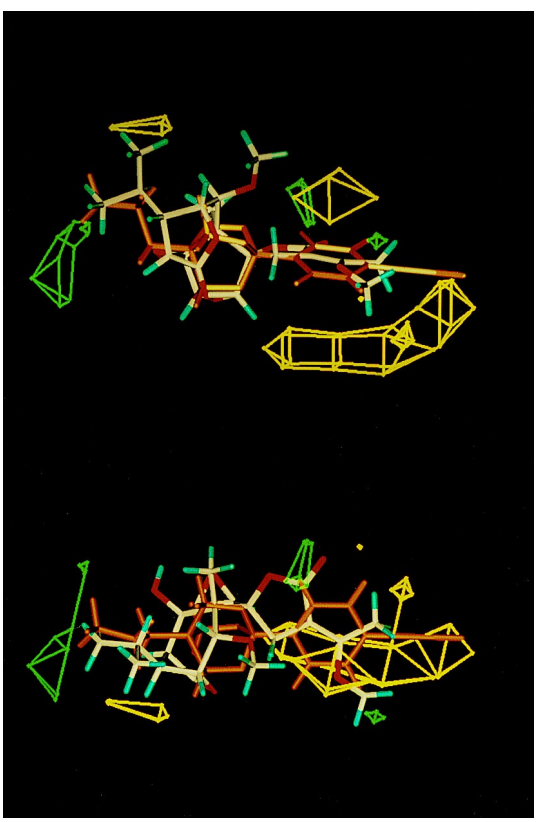

Figure 8. Orthogonal views of contour diagrams of the steric fields according to the CoMFA equation for rat receptors with picrodendrin Q and EBOB (orange).

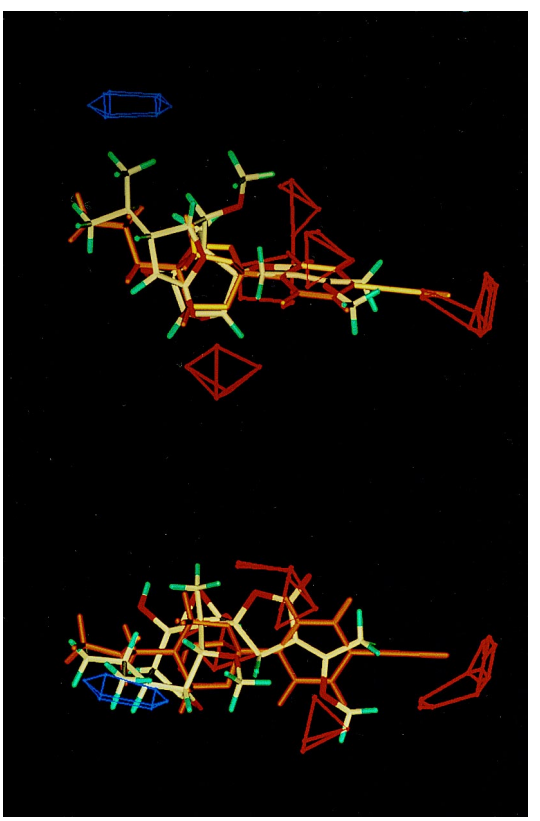

Figure 9. Orthogonal views of contour diagrams of the electrostatic fields according to the CoMFA equation for rat receptors with picrodendrin Q and EBOB (orange).

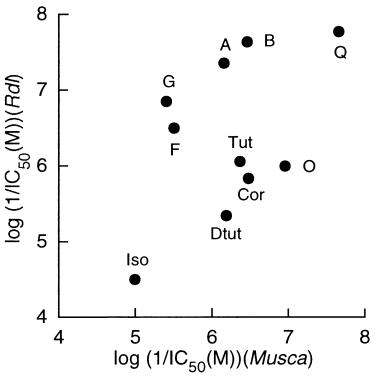

Figure 10. Relationships between the potencies of picrotoxane terpenoids as inhibitors of [^{3}H]EBOB binding to *Musca*-head membranes and antagonists for *Drosophila Rdl* homo-oligomers. *Drosophila* data were taken from ref 15. Abbreviations of the terpenoids' names are defined in Figure 5.

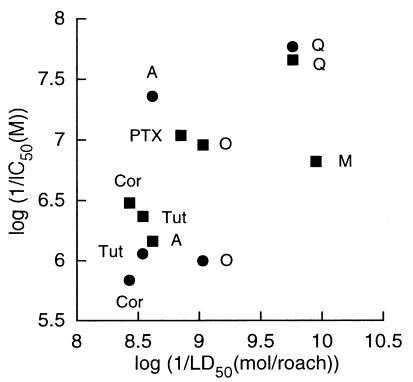

Figure 11. Relationships between the in vivo (abscissa, toxicities against *Blattella*) and in vitro (ordinate, [^{3}H]EBOB binding inhibition in *Musca*-head membranes (■) and GABA-induced Cl^- current block in *Drosophila Rdl* homo-oligomers (●)) activities of picrotoxane terpenoids. Abbreviations of the terpenoids' names are defined in Figure 5.

Musca-head membranes was somewhat disappointing. Despite having IC_{50} values of less than 1 μM, picrodendrin B, E, and corianin showed only weak insecticidal activity. The insecticidal activity of picrodendrin M was higher than expected from the binding assay results. However, the high insecticidal activity of picrodendrin M could be accounted for by bioactivation involving the dehydration of the hydroxyisopropyl group to an isopropenyl group. Omitting these compounds, a reasonable correlation was obtained between the two biological activities ($r = 0.918$). On the other hand, there seems to be no correlation between the activity as antagonists in *Rdl* receptors and the insecticidal activity (Figure 11). Picrodendrin B, F, and G, having IC_{50} values of 0.023, 0.317, and 0.140 μM in *Rdl* receptors, respectively, exhibited only weak insecticidal activities. These findings support the view that native insect GABA receptors contain other subunits,[24] although more studies with the same insect species and by the same functional assays would be needed.

In summary, we have described a series of picrotoxane terpenoids that act as the noncompetitive antagonists of the ionotropic GABA receptors of mammals and insects. The considerable variation in the structures of these terpenoids prevented their detailed quantitative SAR analysis. However, it is clearly demonstrated that the spiro γ-butyrolactone moiety at the 13-position, which contains a carbonyl group conjugated with an unsaturated bond, and the substituents at the 4-position play important roles in the interaction of picrodendrins with the binding site of rat receptors. In contrast, such structural features are not strictly required in the case of the interaction with *Musca* receptors; the spiro saturated γ-butyrolactone moiety at the 13-position, which bears the 16-sp^3 carbon atom, and the hydroxyl groups at various positions (e.g., positions 4 and 8) are somewhat tolerated. Quantitative SAR studies have clearly shown that the electronegativity of the 16-carbon atom and the presence or absence of the 4- and 8-hydroxyl groups are important determinants of the potency of nor-diterpenes in *Musca* receptors, while the negative charge on the 17-carbonyl oxygen atom is likely important in the case of rat receptors. The hydroxyl group at the 4-position is better tolerated in *Drosophila Rdl* homo-oligomers. These findings indicate that there are significant differences between rat and *Musca* native GABA receptors and cloned *Drosophila Rdl* receptors in the structures of their complementary recognition sites. Gurley et al. have reported that the threonine residue at position 246 of β2 subunit is involved in picrotoxinin binding in rat $GABA_A$ receptors containing α1, β2, and γ3 subunits.[27] Xu et al. have reported the possibility that picrotoxinin interacts with the valine residue at position 257 of the α1 subunit in rat $GABA_A$ receptors containing α1, β1, and γ2 subunits.[28] In *Drosophila Rdl* homo-oligomers, replacement of the alanine residue at position 302 with serine confers resistance to picrotoxinin.[29] All of these findings suggest that picrotoxinin binds to a similar pore-facing region of the GABA-gated channels to block the channel. The interacting mechanism of picrotoxane terpenoids with these and other key amino acid residues remains to be identified.

Experimental

Chemicals

Picrodendrin A–J, L–M, O–Q, T, U, X–Z and α, picrodendriside A, dihydrotutin, and isohyenanchin

were isolated from *Picrodendron baccatum* (L.) Krug and Urban.[6–12] Picrodendrin E-18-acetate was obtained by treatment of picrodendrin E with acetic anhydride.[9] Tutin and corianin were isolated from *Coriaria japonica* A. Gray. Picrotoxinin was purchased from Sigma Chemical Co. EBOB was synthesized by the method of Palmer et al.[30] [Propyl-2,3-^{3}H]EBOB (1650.2 GBq/mmol) was purchased from Du Pont/NEN Research Products.

Preparation of rat-brain and *Musca*-head membranes

Rat brain P_2 membranes were prepared from 5-week-old male Wistar rats by a modification of the method of Squires et al.[31] In brief, forebrains stored at −80 °C were thawed and homogenized in ice-cold 1 mM EDTA using a Teflon-glass homogenizer. The homogenate was centrifuged at 1000 *g* for 10 min. The supernatant was then centrifuged at 25,000 *g* for 30 min. The resulting pellet was suspended in 1 mM EDTA and dialyzed three times (2 h each) in cellophane tubing against 2 L of distilled/deionized water at 4 °C. After dialysis, the inner solution was recentrifuged at 25,000 *g* for 30 min, and the pellet was stored at −80 °C until use. The frozen pellet was thawed and suspended in buffer A (300 mM NaCl/10 mM sodium phosphate buffer, pH 7.5) just before the binding assays. *Musca*-head P_2 membranes were prepared from 5- to 10-day-old adult houseflies (*Musca domestica* L.) of WHO strain by a modification of the method of Deng et al.[16] Briefly, the heads were homogenized in 0.25 M sucrose/10 mM Tris-HCl buffer (pH 7.5) with a glass–Teflon homogenizer, filtered through four layers of 64 μm mesh nylon screen and centrifuged at 500 *g* for 5 min. The supernatant was filtered through four layers of nylon screen and centrifuged at 25,000 *g* for 30 min. The pellet was suspended in buffer A and allowed to stand in an ice bath for 30 min. The suspension was centrifuged at 25,000 *g* for 30 min. The pellet was resuspended in buffer A and used immediately for binding assays without freezing.

[^{3}H]EBOB binding assays

[^{3}H]EBOB binding assays were carried out according to Cole and Casida[32] and Deng et al.[16] Briefly, terpenoids were incubated with rat-brain membranes (125 μg protein) or *Musca*-head membranes (250 μg protein) and 0.5 nM [^{3}H]EBOB in 1.0 mL of buffer A at 37 °C for 90 min (rat) or at 22 °C for 70 min (*Musca*). Terpenoids and unlabeled EBOB were added as DMSO solutions (4 μL) to reaction mixtures so as to give the desired final concentrations. After incubation, the mixtures were filtered through GF/B filters and were rapidly rinsed twice with 5 mL of ice-cold buffer A using a Brandel M-24 cell harvester. The radioactivity of [^{3}H]EBOB that specifically bound to membranes on the filters was measured with a Beckman LS 6000SE liquid scintillation spectrometer. Nonspecific binding was determined in the presence of 5 μM unlabeled EBOB. Each experiment was performed in triplicate and repeated twice.

In vivo assays

Acetone solutions (1 μL) of piperonyl butoxide (30 μg) were topically applied to the ventral side of the thorax of male adult German cockroaches (*Blattella germanica* L.). After 1 h, 0.25 μL DMSO solutions containing terpenoids were injected into the ventral portion of the abdomen with a Kloehn microsyringe. After injection, cockroaches were placed in glass vials with water and sugar, and held at 25 °C. One to four groups of 10 cockroaches were used for each dosage. Mortality was recorded 24 h after the injection of terpenoids.

Quantitative SAR analyses

All computations of the molecular modeling were done with the molecular modeling software package SYBYL, version 6.2 and 6.3.[33] To select the initial conformations of compounds, we used X-ray crystallographic coordinates for reference compounds. Those for picrodendrin A and picrodendrin F-18-*p*-bromobenzoate were obtained from the Cambridge Crystallographic Database.[6,9] The coordinates of picrodendrin B, M, Q, and T were modified from those for picrodendrin A. The structures of picrodendrin E, F, G, L, O, P, and E-18-acetate were modeled from the crystal structure of picrodendrin F-18-*p*-bromobenzoate. The coordinates of the modified portions of these structures were calculated using the SYBYL standard values for bond lengths and angles. The initial coordinates thus calculated were fully optimized by the semi-empirical molecular orbital method, PM3.[34–36] For the conformation with the optimized coordinates, the atomic charges were calculated using MNDO.[34,37,38]

Potency in inhibiting [^{3}H]EBOB binding, log ($1/IC_{50}$ (M)), was analyzed by means of the multiple regression technique. The atomic charges and the indicator variable for the presence or absence of the hydroxyl groups at either the 4- or 8-position were used as independent variables.

Superposition of EBOB on picrodendrin Q

A CoMFA average field was defined from the CoMFA fields of four highly active GABA antagonists that appeared in our previous paper;[18] TBOB (4-*t*-butylbicycloorthobenzoate, or 4-*t*-butyl-1-phenyl-2,6,7-trioxabicyclo[2.2.2]octane), H_2BH-1 (5-(4-cyanophenyl)-2,3:8,7-*endo*-4,6-dioxatricyclo[7.2.1.$0^{2,8}$]dodecane), compound 18 (10,11-unsaturated analogue of H_2BH-1), and compound 22 (5-(4-chlorophenyl) analogue of compound 18). The alignment of picrodendrin Q was done

using the Field-fit procedure of SYBYL so that the CoMFA steric and electrostatic fields of picrodendrin Q fit as well as possible in the corresponding CoMFA average fields. EBOB was aligned so that the root mean square of the distances of the atomic positions of the trioxabicyclooctane and benzene rings to the corresponding atomic positions of TBOB was as small as possible.

Acknowledgements

We thank Ms. Hiroko Hasegawa for her assistance in performing in vivo assays.

References

1. Schofield, P. R.; Darlison, M. G.; Fujita, N.; Burt, D. R.; Stephenson, F. A.; Rodriguez, H.; Rhee, L. M.; Ramachandran, J.; Reale, V.; Glencorse, T. A.; Seeburg, P. H.; Barnard, E. A. *Nature* **1987**, *328*, 221.

2. Kaupmann, K.; Huggel, K.; Heid, J.; Flor, P. J.; Bischoff, S.; Mickel, S. J.; McMaster, G.; Angst, C.; Bittiger, H.; Froestl, W.; Bettler, B. *Nature* **1997**, *386*, 239.

3. Barnard, E. A. In *$GABA_A$ Receptors and Anxiety: From Neurobiology to Treatment; Advances in Biochemical Psychopharmacology*; Biggio, G.; Sanna, E.; Serra. M.; Costa, E., Eds.; Raven Press: New York, 1995; Vol. 48, pp 1–16.

4. Johnston, G. A. R. *Pharmacol. Ther*. **1996**, *69*, 173.

5. Sattelle, D. B. *Adv. Insect Physiol*. **1990**, *22*, 1.

6. Ohmoto, T.; Koike, K.; Fukuda, H.; Mitsunaga, K.; Kagei, K.; Kawai, T.; Sato, T. *Chem. Pharm. Bull*. **1989**, *37*, 1805.

7. Ohmoto, T.; Koike, K.; Fukuda, H.; Mitsunaga, K.; Ogata, K.; Kagei, K. *Chem. Pharm. Bull*. **1989**, *37*, 2988.

8. Koike, K.; Fukuda, H.; Mitsunaga, K.; Ohmoto, T. *Chem. Pharm. Bull*. **1991**, *39*, 934.

9. Koike, K.; Ohmoto, T.; Kawai, T.; Sato, T. *Phytochemistry* **1991**, *30*, 3353.

10. Suzuki, Y.; Koike, K.; Ohmoto, T. *Phytochemistry* **1992**, *31*, 2059.

11. Koike, K.; Suzuki, Y.; Ohmoto, T. *Phytochemistry* **1994**, *35*, 701.

12. Nagahisa, M.; Koike, K.; Narita, M.; Ohmoto, T. *Tetrahedron* **1994**, *50*, 10859.

13. Hayden, W. J.; Gillis, W. T.; Stone, D. E.; Broome, C. R.; Webster, G. L. *J. Arnold Arbor*. **1984**, *65*, 105.

14. Ozoe, Y.; Hasegawa, H.; Mochida, K.; Koike, K.; Suzuki, Y.; Nagahisa, M.; Ohmoto, T. *Biosci. Biotech. Biochem*. **1994**, *58*, 1506.

15. Hosie, A. M.; Ozoe, Y.; Koike, K.; Ohmoto, T.; Nikaido, T.; Sattelle, D. B. *Br. J. Pharmacol*. **1996**, *119*, 1569.

16. Deng, Y.; Palmer, C. J.; Casida, J. E. *Pestic. Biochem. Physiol*. **1993**, *47*, 98.

17. Ozoe, Y.; Kuwano, E.; Eto, M. *Biosci. Biotech. Biochem*. **1993**, *57*, 504.

18. Akamatsu, M.; Ozoe, Y.; Ueno, T.; Fujita, T.; Mochida, K.; Nakamura, T.; Matsumura, F. *Pestic. Sci*. **1997**, *49*, 319.

19. Cramer, R. D., III; Patterson, D. E.; Bunce, J. D. *J. Am. Chem. Soc*. **1988**, *110*, 5959.

20. Eto, M.; Ozoe, Y.; Fujita, T.; Casida, J. E. *Agr. Biol. Chem*. **1976**, *40*, 2113.

21. ffrench-Constant, R. H.; Mortlock, D. P.; Shaffer, C. D.; MacIntyre, R. J.; Roush, R. T. *Proc. Natl. Acad. Sci. U.S.A*. **1991**, *88*, 7209.

22. Henderson, J. E.; Soderlund, D. M.; Knipple, D. C. *Biochem. Biophys. Res. Commun*. **1993**, *193*, 474.

23. Harvey, R. J.; Schmitt, B.; Hermans-Borgmeyer, I.; Gundelfinger, E. D.; Betz, H.; Darlison, M. G. *J. Neurochem*. **1994**, *62*, 2480.

24. Hosie, A. M.; Sattelle, D. B. *Br. J. Pharmacol*. **1996**, *117*, 1229.

25. Hosie, A. M.; Sattelle, D. B. *Br. J. Pharmacol*. **1996**, *119*, 1577.

26. Thompson, M.; Steichen, J. C.; ffrench-Constant, R. H. *Insect Mol. Biol*. **1993**, *2*, 149.

27. Gurley, D.; Amin, J.; Ross, P. C.; Weiss, D. S.; White, G. *Recept. Channels* **1995**, *3*, 13.

28. Xu, M.; Covey, D. F.; Akabas, M. H. *Biophys. J*. **1995**, *69*, 1858.

29. ffrench-Constant, R. H.; Rocheleau, T. A.; Steichen, J. C.; Chalmers, A. E. *Nature* **1993**, *363*, 449.

30. Palmer, C. J.; Cole, L. M.; Larkin, J. P.; Smith, I. H.; Casida, J. E. *J. Agric. Food Chem*. **1991**, *39*, 1329.

31. Squires, R. F.; Casida, J. E.; Richardson, M.; Saederup, E. *Mol. Pharmacol*. **1983**, *23*, 326.

32. Cole, L. M.; Casida, J. E. *Pestic. Biochem. Physiol*. **1992**, *44*, 1.

33. SYBYL Molecular Modeling Software, Tripos Associates, Inc., St. Louis, MI.

34. Stewart, J. J. P. MOPAC Ver.5, Quantum Chemistry Program Exchange, Program no. 455, Indiana University, Bloomington, IN.

35. Stewart, J. J. P. *J. Compt. Chem*. **1989**, *10*, 209.

36. Stewart, J. J. P. *J. Compt. Chem*. **1989**, *10*, 221.

37. Dewar, M. J. S.; Thiel, W. *J. Am. Chem. Soc*. **1977**, *99*, 4899.

38. Dewar, M. J. S.; Thiel, W. *J. Am. Chem. Soc*. **1977**, *99*, 4907.